

Triggered star formation in expanding shells

S. Ehlerová^{*} and J. Palouš[†]

Astronomical Institute, Academy of Sciences of the Czech Republic, Boční II 1401, 141 31 Prague 4, Czech Republic

Received 2001 August 6 / Accepted 2001 November 13

ABSTRACT

We discuss fragmentation processes which induce star formation in dense walls of expanding shells. The influence of the energy input, the ISM scale-height and speed of sound in the ambient medium is tested. We formulate the condition for the gravitational fragmentation of expanding shells: if the total surface density of the disc is higher than a certain critical value, shells are unstable. The value of the critical density depends on the energy of the shell and the sound speed in the ISM.

Key words: Stars: formation – ISM: bubbles – ISM: structure

1 INTRODUCTION

HI shells (or supershells) are structures identified in the distribution of the neutral hydrogen (HI) in the Milky Way and in many nearby galaxies. The typical shell consists of a rarefied medium surrounded by a dense thin wall, in some cases expanding supersonically to the ambient interstellar medium (ISM). Dimensions of shells lie in the range from a few 10 pc to a few kpc. Energies involved in their creation are of the order of $10^{50} - 10^{54}$ erg. Shells have miscellaneous shapes, but many of them are nearly spherical, elliptical or cylindrical. Observations of shells are reviewed in Brinks & Walter (1998).

The energy needed for the creation of a shell originates either in the combined effect of massive stars in an OB association (radiation, stellar winds and supernova explosions), in the very energetic event connected to the gamma-ray burst (a hypernova or merging of compact companions in a binary system), or in the infall of a high velocity cloud (HVC) to the galactic HI disc. In this paper we consider the continuous energy input from massive stars of an OB association.

The density of the swept-up gas in walls of shells is higher than the average density of the unperturbed ambient medium, which increases the probability of star formation. Star formation in dense walls of HI shells is observed in some galaxies, e.g. in LMC (Kim et al., 1999), SMC (Stanimirovic et al., 1999), IC 2574 (Walter & Brinks, 1999), Sex A (Van Dyk et al. 1998), etc. Its significance for the evolution of galaxies was studied by Palouš et al. (1994) and others.

There are different mechanisms to trigger star formation: (1) a compression of pre-existing clouds, (2) an accumulation of gas into a shell, (3) cloud collisions (Elmegreen,

1998), (4) shell collisions (Chernin et al., 1995). Here we focus on the mechanism (2) of the gravitational instability of mass accumulated in a thin expanding shell. The growth of perturbations was analyzed in the linear approximation by Elmegreen (1994), nonlinear terms have been included by Wünsch & Palouš (2001).

Any density perturbation on the shell surface is stretched by the expansion, while its self-gravity supports its growth. The instantaneous maximum growth rate is

$$\omega = -\frac{3V}{R} + \sqrt{\frac{V^2}{R^2} + \left(\frac{\pi G \Sigma_{sh}}{c_{sh}}\right)^2}, \quad (1)$$

where R is the radius of the shell, V is its expansion speed, Σ_{sh} is its column density and c_{sh} is the speed of sound within the wall. The perturbation grows only if $\omega > 0$.

In galaxies with thin discs shells differ from a sphere. To discuss star formation triggered in expanding shells without an a priori assumption on their shapes, we use 3-dimensional simulations. In a numerical code, the condition (1) is used and we quantify when and where the expanding shell starts to be unstable. This approach was first used in Ehlerová et al. (1997, Paper I), here we extend parameter ranges and generalize results. We also discuss triggered star formation observed in nearby galaxies and its connection to expanding shells.

2 THE THIN SHELL APPROXIMATION

The energy input from an OB association creates a blast-wave, which propagates into the ambient medium (Ostriker & McKee 1988; Bisnovatyi-Kogan & Silich 1995). During the majority of the evolution its radius is much larger than its thickness and the thin shell approximation can be used. In this approximation the blastwave is considered to be

^{*} E-mail: sona@ig.cas.cz

[†] E-mail: palous@ig.cas.cz

an expanding infinitesimally thin layer surrounding the hot medium inside.

2.1 The analytical solution

The analytical solution of the expansion in the thin shell approximation was derived by Sedov (1959). In a static, homogeneous medium without the external or internal gravitational field, the blastwave is always spherically symmetric, it sweeps the ambient matter and decelerates. Neglecting the external pressure, and assuming the continuous energy input L , the self-similar solution for R , V and Σ_{sh} is (Castor et al., 1975):

$$R(t) = 53.1 \times \left(\frac{L}{10^{51} \text{ erg Myr}^{-1}} \right)^{\frac{1}{5}} \times \left(\frac{\mu}{1.3 \text{ cm}^{-3}} \frac{n}{\text{cm}^{-3}} \right)^{-\frac{1}{5}} \times \left(\frac{t}{\text{Myr}} \right)^{\frac{3}{5}} \text{ pc}, \quad (2)$$

$$V(t) = 31.2 \times \left(\frac{L}{10^{51} \text{ erg Myr}^{-1}} \right)^{\frac{1}{5}} \times \left(\frac{\mu}{1.3 \text{ cm}^{-3}} \frac{n}{\text{cm}^{-3}} \right)^{-\frac{1}{5}} \times \left(\frac{t}{\text{Myr}} \right)^{-\frac{2}{5}} \text{ km s}^{-1}, \quad (3)$$

$$\Sigma(t)_{sh} = 0.564 \times \left(\frac{L}{10^{51} \text{ erg Myr}^{-1}} \right)^{\frac{1}{5}} \times \left(\frac{\mu}{1.3 \text{ cm}^{-3}} \frac{n}{\text{cm}^{-3}} \right)^{\frac{4}{5}} \times \left(\frac{t}{\text{Myr}} \right)^{\frac{3}{5}} M_{\odot} \text{ pc}^{-2}, \quad (4)$$

where n and μ are the volume particle density of the ambient medium and the relative weight of one particle (see also Paper I or Ehlerová, 2000).

The formula (1) for the instantaneous maximum growth rate of perturbations shows that at early stages of the evolution the shell is stable, as the fast expansion stretches all perturbations which might appear. Only later, when V is small, R large and Σ_{sh} high, the self-gravity starts to play a role. At the time t_b , when the growth rate ω becomes positive for the first time, the shell starts to be unstable and the fragmentation process begins.

Inserting the analytical solution (2) - (4) for R , V and Σ_{sh} to the formula (1) we get relations for the time t_b , the radius $R(t_b)$ and the expansion velocity $V(t_b)$:

$$t_b = 28.8 \times \left(\frac{c_{sh}}{\text{km s}^{-1}} \right)^{\frac{5}{8}} \times \left(\frac{L}{10^{51} \text{ erg Myr}^{-1}} \right)^{-\frac{1}{8}} \times \left(\frac{\mu}{1.3 \text{ cm}^{-3}} \frac{n}{\text{cm}^{-3}} \right)^{-\frac{1}{2}} \text{ Myr}, \quad (5)$$

$$R(t_b) = 399 \times \left(\frac{c_{sh}}{\text{km s}^{-1}} \right)^{\frac{3}{8}} \times \left(\frac{L}{10^{51} \text{ erg Myr}^{-1}} \right)^{\frac{1}{8}} \times \left(\frac{\mu}{1.3 \text{ cm}^{-3}} \frac{n}{\text{cm}^{-3}} \right)^{-\frac{1}{2}} \text{ pc}, \quad (6)$$

$$V(t_b) = 8.13 \times \left(\frac{c_{sh}}{\text{km s}^{-1}} \right)^{-\frac{1}{4}}$$

$$\times \left(\frac{L}{10^{51} \text{ erg Myr}^{-1}} \right)^{\frac{1}{4}} \text{ km s}^{-1}. \quad (7)$$

The radius $R(t_b)$ is a lower limit to the distance on which the fragmentation (and triggered star formation) may happen; the expansion velocity $V(t_b)$ is the expansion velocity at which the fragmentation process begins. Since in the subsequent evolution the shell further decelerates it gives the upper limit to the random component of the velocity of newly created clouds (or stars). The relation (7) shows that $V(t_b)$ does not depend on the density of the ambient medium n . This may be one reason why new clouds are born in different environments with similar velocity dispersions.

Relations (5), (6) and (7) are derived under the assumption of the supersonic motion, i.e. $v_{exp}(t) > c_{ext}$. If the shell becomes a sound wave before it starts to be unstable (i.e. before the time t_b), it will always remain stable. Assuming that the expansion velocity V at t_b has to be greater than or equal to the sound speed in the ambient medium c_{ext} , we can derive from the equation (7) the critical luminosity of the energy source L_{crit} , for which the expansion velocity V at the time t_b equals the sound speed c_{ext} :

$$L_{crit} = \left(\frac{c_{ext}}{8.13 \text{ km s}^{-1}} \right)^4 \left(\frac{c_{sh}}{\text{km s}^{-1}} \right) 10^{51} \text{ erg Myr}^{-1} \quad (8)$$

If the energy input is greater than L_{crit} , the shell starts to fragment; if the input is smaller, the shell is always stable. L_{crit} does not depend on the density of the ambient medium but it is a strong function of its speed of sound.

Relations (5), (6) and (7), which apply to the static and homogeneous ambient medium, can be extended to spherically symmetric cases with the density gradient. Theis et al. (1998) show, that the density gradient in the surrounding medium has to be shallower than isothermal for the self-gravity of the accumulated matter to overcome the stability supported by the expansion.

The analytical solution for shells expanding in the exponentially stratified ISM was derived by Maciejewski and Cox (1999). It assumes that the shape of the shell can be approximated by a prolate ellipsoid. This assumption applies only to small shells created by energies corresponding to about one supernova in the special ISM distribution. Unfortunately, for supershells with energies in the range $10^{52} - 10^{54}$ erg, the assumption of ellipticity fails.

The linear perturbation theory does not estimate the evolution of the instability after the time t_b very well. A better estimate of the evolution at $t > t_b$ is provided by the analysis including nonlinear terms (Wünsch & Palouš, 2001).

2.2 Numerical simulations

The thin shell approximation has been applied in numerical simulations in one and two dimensions by many authors (see Ikeuchi, 1998, for a review on this subject). Models have been further extended into three dimensions by Palouš (1990) and Silich et al. (1996).

The code, which we use in this paper, is an improved and extended successor to the code of Palouš (1990), described in Paper I and in Efremov et al. (1999). The thin shell is divided into a number of elements; a system of equa-

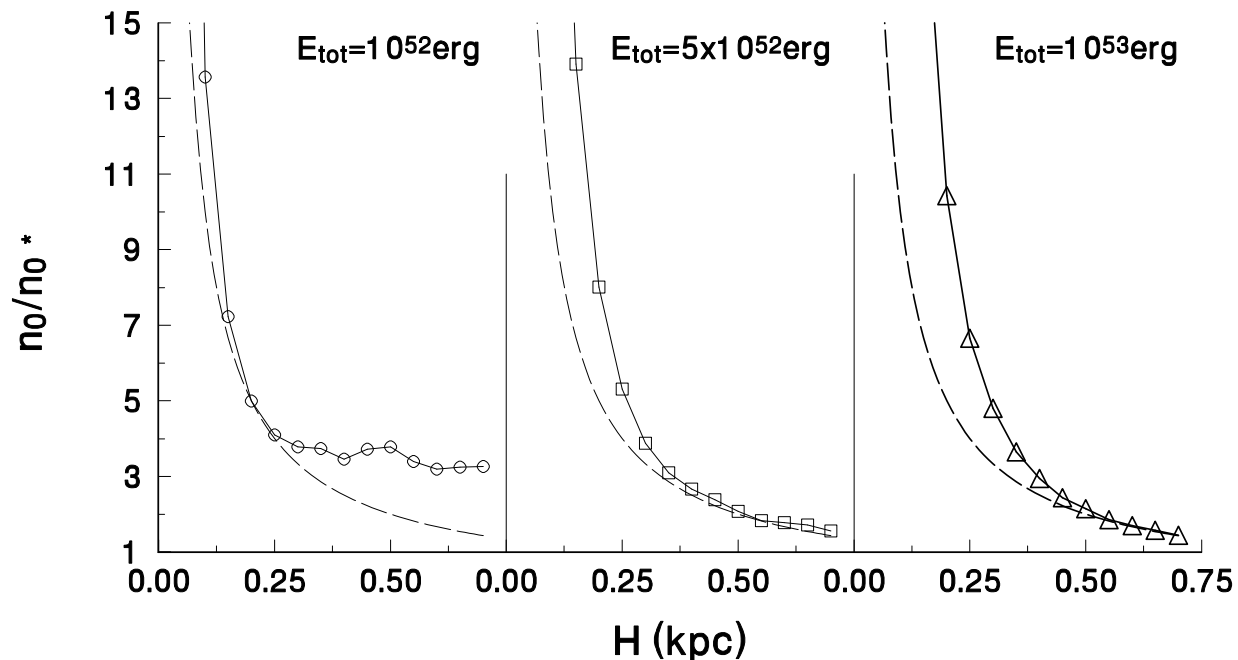


Figure 1. Fragmentation of shells in Gaussian discs, $c_{ext} = 5 \text{ km s}^{-1}$. The total input energy E_{tot} is given in each panel. The normalization density parameter $n_0^* = 0.265 \text{ cm}^{-3}$ (left panel); 0.056 cm^{-3} (center); 0.031 cm^{-3} (right panel). Results of numerical simulations are shown by symbols connected by solid lines, they show the minimum density n_0 needed for the onset of the fragmentation. Dashed lines correspond to the constant gas surface density $\Sigma_{gas} = 14.5 \times 10^{20} \text{ cm}^{-2}$ (left panel); $3.1 \times 10^{20} \text{ cm}^{-2}$ (center); $1.7 \times 10^{20} \text{ cm}^{-2}$ (right panel).

tions of motion, mass and energy for each element is solved and the fragmentation condition (1) is evaluated.

Numerical simulations include some effects, which are neglected in the analytical solution. The most important are: 1) the pressure of the ambient medium and radiative cooling; 2) the finite, time-limited energy input from an OB association (life-time of the source is τ , we take $\tau = 15 \text{ Myr}$); and perhaps the most obvious one 3) the stratification of the ISM in galaxies.

Due to the disc-like ISM density distribution and to the form of the gravitational potential, shapes of expanding shells are not spherical, but elongated in the direction of the density gradient; the differential rotation distorts shells in the plane parallel to the galactic plane. In the case of higher input energies and thin discs, a blow-out may occur and a fraction of the energy supplied by hot stars escapes to the galactic halo. Blow-out decreases the influence of the energy source on the densest parts of the shell in the galactic plane.

Fragmentation properties vary with the position on the shell. Typically, for shells growing in a smooth distribution of gas with the z -gradient, a dense ring is created in the region of the maximum density. This is the most unstable part of the shell, while large lobes in low-density regions are stable. In the following we present results for the most unstable part of shells. Energy sources, which are not located in the symmetry plane of the disc, produce asymmetrical shells. However, as the fragmentation takes place in the densest

regions, it is not influenced very much by the asymmetry of the shell. The blow-out effects (and the subsequent decrease of the “effective” energy) are enhanced in such a case.

The gravitational field of the galaxy may change the velocity field of the ISM and the shape of the shell, and thus conditions for the fragmentation. Simulations show, that the differential rotation has a smaller influence than the density stratification. Usually, two unstable regions appear on tips of an ellipse. Galaxies with little shear (e.g. dwarfs) do not influence the shells even to that degree (see Ehlerová, 2000).

The ISM in galaxies is not perfectly smooth but contains many small-scale density fluctuations (see Silich et al, 1996, for the partial analysis of their influence), it is turbulent etc. However, coherent shells and bubbles are observed even in a rather turbulent ISM. Our numerical experiments in a medium with a hierarchy of density fluctuations show, that shells are mostly influenced by the large-scale gradients in the ISM (with the possible exception of the very perturbed regions, where the coherent shock does not form).

3 THE CRITICAL SURFACE DENSITY

To study the influence of the z -stratification, we simulate shells in different types of the ISM distribution with different disc thicknesses. We fix the velocity dispersion in the shell c_{sh} (see eq. 1) to a constant value: $c_{sh} = 1 \text{ km s}^{-1}$. Results

for the Gaussian stratification $n(z) = n_0 e^{-z^2/H^2}$ are given in Fig. 1. Symbols denoting different E_{tot} show the lowest density n_0 needed for the onset of the instability during the shell expansion. For a given disc thickness H , a total energy E_{tot} (E_{tot} is the total energy delivered by the OB association to the shell: $E_{tot} = L \times \tau$) and a velocity dispersion c_{ext} , shells are unstable only if n_0 exceeds the depicted value. For lower values shells remain stable. Dashed lines are lines of the constant gas surface density in the disc (Σ_{gas}).

As can be seen in Fig. 1, lines of the constant disc surface density Σ_{gas} approximately separate stable and unstable regions. There are two types of deviations between the solid line separating stable and unstable regions and $\Sigma_{gas} = const$ line:

- **The blow-out effect.** It is visible in the middle and right panels (i.e. in the case of higher energies) for thin discs: a higher density n_0 is needed for the instability than predicted by $\Sigma_{gas} = const$. The blow-out enables the leakage of the energy to the galactic halo, leading to the decrease of the effective energy and pressure pushing the densest parts of the shell.

- **The small shell in the thick disc.** It is visible in the left panel (i.e. in the case of a low energy) and thick discs: a higher value of n_0 than predicted by $\Sigma_{gas} = const$ line is needed for the instability. Low energy shells are generally small and in thick discs they evolve in an almost homogeneous medium as they never reach dimensions comparable to the thickness of the disc. Consequently, the value of the gas surface density of the disc is irrelevant. The critical value of n_0 has to be higher than predicted by $\Sigma_{gas} = const$ criterion, since a substantial fraction of the ISM in the disc remains untouched by the shell.

A different behavior is observed in complementary simulations with $\tau = \infty$ (long-lasting energy supply). In this case shells fragment at a radius $R(t_b) \simeq 1.5H$. Inserting this condition into eq. (6) we get $n_0 \propto 1/H^2$ for given c_{sh} and L . The deviation from this behavior in Fig. 1 is connected to the fact that $\tau < t_b$.

Other simulations with different disc profiles (Gaussian, exponential, multicomponent) show that the critical value of the gas surface density Σ_{crit} does not depend on the profile. Σ_{crit} depends strongly on c_{ext} : for higher values of c_{ext} the fragmentation starts at higher values of Σ_{gas} . We derive the fit:

$$\Sigma_{crit} = 0.27 \left(\frac{E_{tot}}{10^{51} \text{erg}} \right)^{-1.1} \left(\frac{c_{ext}}{\text{km s}^{-1}} \right)^{4.1} 10^{20} \text{cm}^{-2}. \quad (9)$$

This relation is illustrated in Fig. 2.

4 COMPARISON TO OBSERVATIONS

In this paragraph we study one example of the HI hole with star formation on the rim. This is the structure number 35 in the galaxy IC 2574 (Walter & Brinks, 1999). Taking the measured value of $c_{ext} = 7 \text{ km s}^{-1}$ and the total energy input from stellar winds and supernovae of the central star cluster inside this shell, estimated by Stewart & Walter (2000) as $E_{tot} = 4.1 \times 10^{52} \text{erg}$, and using the formula (9) we derive the critical gas surface density $\Sigma_{crit} = 1.3 \times 10^{21} \text{cm}^{-2}$. The gas surface density in the vicinity of this shell, $1.8 \times 10^{21} \text{cm}^{-2}$

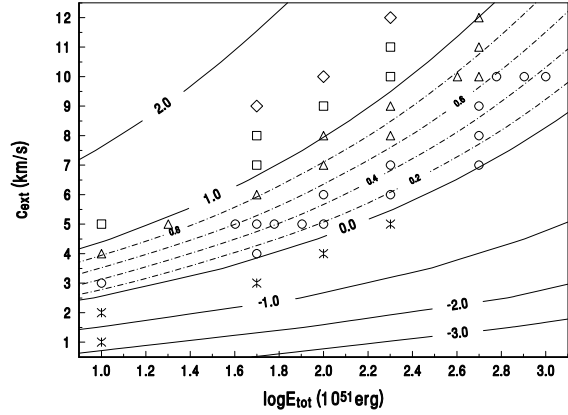


Figure 2. The critical gas surface density Σ_{crit} in the $(\log E_{tot}, c_{ext})$ plane. Various symbols show Σ_{crit} from numerical experiments: * = $\Sigma_{crit} \leq 10^{20} \text{cm}^{-2}$; o = $10^{20} < \Sigma_{crit} \leq 4 \times 10^{20}$; $\Delta = 4 \times 10^{20} < \Sigma_{crit} \leq 10^{21}$; $\square = 10^{21} < \Sigma_{crit} \leq 2 \times 10^{21}$; $\diamond = 2 \times 10^{21} < \Sigma_{crit}$. Contour lines are calculated by the formula (9) and labelled by the logarithm of Σ_{crit} in 10^{20}cm^{-2} .

Name	c_{ext} km s^{-1}	Σ_{crit}^{obs} $M_{\odot} \text{pc}^{-2}$	E_{tot} 10^{51}erg
IC 1613	7.5	3	257
Ho II	6.8	6	92
DDO 155	9.5	3	640

Table 1. Values of the minimum input energy to trigger star formation on the rim of the shell, E_{tot} , as derived from the observed values of c_{ext} and Σ_{crit}^{obs} .

(as given by Walter & Brinks 1999), is higher than the derived value Σ_{crit} , which is consistent with our hypothesis.

We may derive $R(t_b)$ using formula (6) for a homogeneous medium. For this hole we get $R(t_b) \sim 500 \text{ pc}$, which is quite close to the observed dimension. The disc thickness H of IC 2574 is 350 pc, which is less than $R(t_b)$, and the assumption of homogeneity is not fulfilled. In our opinion, the condition (9) is more suitable for a discussion of the fragmentation process since it takes into account the z -stratification.

A comparison of the HI distribution in IC 2574 to the H_{α} emission (which is very often connected to rims of HI shells) suggests, that majority of H_{α} emission lies in the regions with $\Sigma_{gas} \geq 1.7 \times 10^{21} \text{cm}^{-2}$. If this is the critical gas surface density Σ_{crit} , we can estimate the value of the minimum energy necessary to produce an unstable shell, which is $E_{tot} = 3.8 \times 10^{52} \text{erg}$. It means, that in IC 2475 clusters with ~ 40 massive stars and more can trigger star formation.

In Table 1 we show the observed average value of the velocity dispersion c_{ext} and Σ_{crit}^{obs} , the azimuthally averaged value of the gas surface density, below which star forma-

tion rate strongly declines, for three galaxies selected from Hunter et al. (1998). E_{tot} in the last column of Table 1, derived from the formula (9), gives the value of the minimum input energy necessary to create an unstable expanding shell. Corresponding numbers of massive stars in the star cluster differ for different galaxies: in IC 2574 and Ho II less numerous clusters than in IC 1613 and DDO 155 are needed.

5 CONCLUSIONS

We study the gravitational instability of expanding shells using the analytical solution and numerical simulations. The influence of the total energy E_{tot} , the velocity dispersion of the ISM c_{ext} , the thickness and the profile of the gaseous disc are analyzed with the following result: the critical value of the disc gas surface density Σ_{crit} exists; shells expanding in discs with the lower gas surface density are stable, shells expanding in discs with the higher density are unstable, can fragment and form gaseous clouds and later stars.

Values of Σ_{crit} for reasonable values of E_{tot} and c_{ext} are of the order of $(10^{20} - 10^{21}) \text{ cm}^{-2}$, which coincides with the value of observed threshold surface densities for star formation in galaxies (Kennicutt, 1997, 1998; Hunter et al., 1998). This agreement may indicate, that the contribution of star formation induced by shells to total star formation is important.

We should distinguish between two cases: 1) the gas surface density Σ_{gas} in the shell is increased compared to the average, which decreases the value of Toomre (1964) or Safronov (1960) parameter Q for the local gravitational instability of the galactic disc; 2) the material accumulated in the shell starts to be unstable according to the formula (1). We label the first case an enhanced mechanism of spontaneous star formation, the second case describes triggered star formation. According to our simulations, the main difference lies in the dependence on the velocity dispersion in the unperturbed medium c_{ext} : the critical density Σ_{crit} is in the case of spontaneous star formation directly proportional to c_{ext} , but in the case of triggered star formation it depends on c_{ext}^4 . A much sharper dependence of Σ_{crit} on c_{ext} is connected to the mass accumulation to the shell, which stops when the shell decelerates to c_{ext} .

The very steep dependence of Σ_{crit} on c_{ext} indicates the importance of the self-regulating feedback for triggered star formation mode. Young stars in OB associations release the energy and compress the ambient ISM creating shells. In dense walls of shells, star formation may be triggered if the disc surface density surpasses a critical value Σ_{crit} . Star formation is accompanied by the heating of the ISM, i.e. increasing c_{ext} . This leads to the increase of Σ_{crit} and a subsequent reduction of triggered star formation rate. The energy dissipation and cooling of the ISM decreases c_{ext} and Σ_{crit} and increases star formation, closing the self-regulating cycle of the triggered mode of star formation.

The heating of the ISM and the increase of c_{ext} related to star formation is a localized process operating on scales of $100 \text{ pc} - 1 \text{ kpc}$ in size. Consequently, triggered star formation is a more local process than the spontaneous mode. The less steep dependence of Σ_{crit} on c_{ext} for spontaneous star formation means, that this mode may be also effective in

regions, where c_{ext} is increased and the triggered mode of star formation temporarily stopped.

ACKNOWLEDGEMENTS

We would like to thank B. G. Elmegreen, L. S. Schulman and to anonymous referee for helpful comments. Authors gratefully acknowledge a financial support by the Grant Agency of the Academy of Sciences of the Czech Republic under the grant No. A3003705/1997 and a support by the grant project of the Academy of Sciences of the Czech Republic No. K1048102.

REFERENCES

- Bisnovatyi-Kogan G.S., Silich S.A., 1995 Rev. Mod. Phys. 67, 661
 Brinks E., Walter F., 1998, in The Magellanic Clouds and Other Dwarf Galaxies, ed. T. Richtler, J.M. Braun, Shaker Verlag, p. 1
 Castor J., McCray R., Weaver R., 1975, ApJ 200, L107
 Chernin, A. D., Efremov, Yu. N., Voinovich, P. A., 1995, MNRAS 275, 313
 Efremov Yu.N., Ehlerová S., Palouš J., 1999, A&A 350, 457
 Ehlerová S., 2000, PhD Thesis, Charles University, Prague
 Ehlerová S., Palouš J., Theis Ch., Hensler G., 1997, A&A 328, 121, Paper I
 Elmegreen B. G., 1994, ApJ 427, 384
 Elmegreen B. G., 1998, in Origins of Galaxies, Stars, Planets and Life, ed. C. E. Woodward, H. A. Thronson, & M. Shull, ASP Conf. Ser. 148, p. 150
 Hunter D.A., Elmegreen B. G., Baker A.L., 1998, ApJ 493, 595
 Ikeuchi S., 1998, in The Local Bubble and Beyond (IAU Colloquium No. 166), eds. D. Breitschwerdt, M.J. Freyberg, J. Trümper, Springer-Verlagp. 399-408
 Kennicutt, R.C., 1997, in The Interstellar Medium in Galaxies, ed. J. M. van der Hulst, Kluwer Academic Publishers, p. 171
 Kennicutt R.C., 1998, ApJ 498, 541
 Kim S., Dopita M. A., Staveley-Smith L., Bessell M. S., 1999, AJ 118, 2797
 Maciejewski W., Cox, D. P., 1999, ApJ 511, 792
 Ostriker J.P., Mc Kee C.F., 1988, Rev. Mod. Phys. 60, 1
 Palouš J., 1990, in The Interstellar Disk-Halo Connection in Galaxies, ed. H. Bloemen, Sterrewacht Leiden, The Netherlands, p. 101
 Palouš J., Tenorio-Tagle G., Franco J., 1994, MNRAS 270, 75
 Safronov V. S., 1960, Annales d'Astrophysique 23, 979
 Sedov L., 1959, Similarity and Dimensional Methods in Mechanics, Academy Press, New York
 Silich S.A., Franco J., Palouš J., Tenorio-Tagle G., 1996, ApJ 468, 722
 Stanimirovic S., Staveley-Smith L., Dickey J. M., Sault R. J., Snowden S. L., 1999, MNRAS 302, 417
 Stewart S. G., Walter F., 2000, AJ, submitted
 Theis, Ch., Ehlerová, S., Palouš, J., Hensler G., 1998, in The Local Bubble and Beyond, Springer Verlag, eds. D. Breitschwerdt, M. J. Freyberg, and J. Trümper, p. 409
 Toomre A., 1964, ApJ 139, 1217
 Van Dyk S.D., Puche D., Wong T., 1998, 116, 2341
 Vishniac E. T., 1994, ApJ 428, 186
 Walter F., Brinks E., 1999, AJ 118, 273
 Wünsch R., Palouš J., 2001, A&A, 374, 746